Mirror jitter: an overview of theoretical and experimental work

Michael J. Laughlin
8687 Kelso Drive
Palm Beach Gardens, Florida 33418

Abstract. Mirror jitter is a flow-induced vibration phenomenon typical of convectively cooled optics. Flow separation points within the coolant supply lines, mirror manifolding, and mirror coolant passages produce internal turbulent pressure distributions, which lead to unbalanced fluctuating forces and resultant mirror jitter. The author reviews the known causes of jitter, methods to determine jitter forces as well as actual mirror jitter, and methods to measure jitter forces. A summary of known jitter force measurements is given, and an extensive bibliography of relevant literature is listed. Guidelines for evaluating system jitter and avoiding pitfalls are offered.

Subject terms: high heat flux; mirror jitter; flow separation points; mount design.

Optical Engineering 34(2), 321–329 (February 1995).

1 Introduction

Mirrors intended to control a high-intensity electromagnetic beam are generally cooled with internal coolant passages to control thermal distortion. Figure 1 shows a typical design that includes an entrance and exit tube and manifold areas that lead into and out of smaller, high-flow-rate coolant passages constituting a heat exchanger. The heat loads induced by the electromagnetic beam require flow rates in the coolant passages such that each local Reynolds number is well above the critical level required to produce turbulent flow. Turbulent flow is characterized by velocity fluctuations and hence pressure fluctuations. Whereas the mean and all fluctuating components of the velocity are forced to vanish at the passage walls, the pressure fluctuations at the wall are comparable to those throughout the flowfield. As a consequence the local wall pressure fluctuations combine in an integral sense to produce a net "jitter" force on the mirror. In addition, the flow passages within the mirror include regions of local flow separation. Separated flow results in large-scale eddy circulation that produces turbulent flow in which the pressure fluctuations may be several orders of magnitude larger than those characteristic of fully developed turbulent flow in a tube. Thus, in order to understand and predict the fluctuating force produced by the coolant flow, one must predict the position and spatial scale of flow separation. The fluctuating force is reacted by the mount supporting the mirror. The flexibility of the mount results in dynamic jitter motion of the mirror.

Paper HHF-01 received Aug. 4, 1994, revised manuscript received Nov. 2, 1994; accepted for publication Nov. 2, 1994.

With the exception of acoustic excitation, cavitation, and fluid-elastic coupling effects, a general procedure is developed that will calculate the net jitter force and vibration response produced by the coolant flow, based on dimensionless data found in the open literature. As a consequence, it identifies the required parameters necessary to describe the force and response, and demonstrates the influence of each parameter and of variations in the flow configuration. Based on this information, several design techniques are presented that can be implemented to reduce the mirror jitter response. These techniques are aimed at reducing the magnitude of the forcing function and reducing the magnitude of the mirror-mount response to a given force. This report discusses how coolant-flow-induced forces and motions that have actually been measured and reported have provided a broad data base and allowed verification of jitter predictions. Finally, a mirror-mount system design example is presented, which illustrates how the aspects of vibration control discussed in this paper are integrated into the design of a high-performance optic.

2 Flow-Induced Jitter Force

The theoretical development of the procedure for evaluating the coolant-flow-induced force, as explained below, was carried out by Dr. R. K. Irey, University of Florida, Gainesville, working as a consultant for United Technologies Research Center (UTRC) in the summer of 1982.[1] Dr. Irey reviewed a large volume of technical literature for relevance to the subject of coolant-flow-induced forces; those that supported the development are cited in Ref. 1, and are reprinted herein for completeness.[2–65] A summary of that work, along with much of the application technology developed at the UTRC, is given in the following paragraphs.

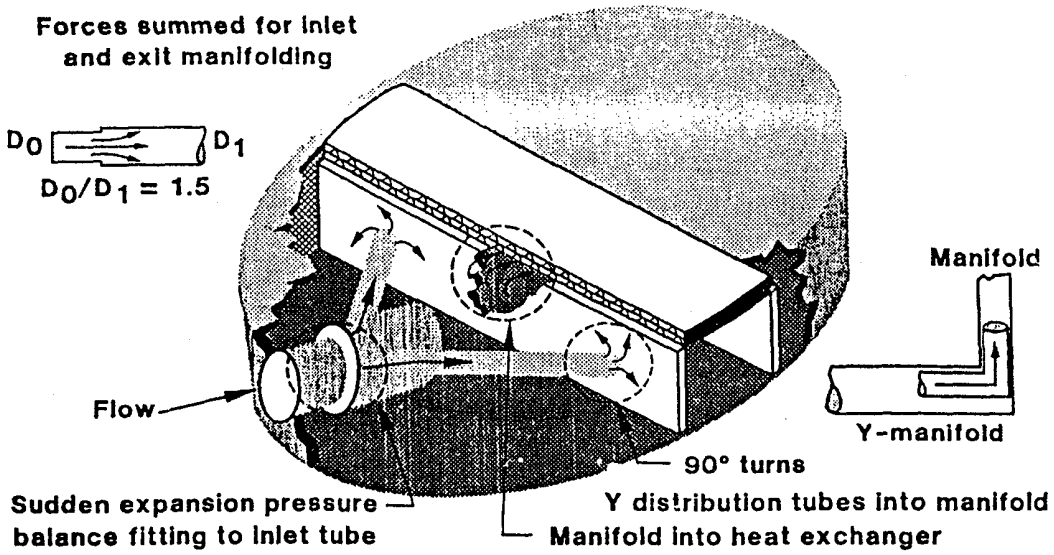

Fig. 1 Typical mirror geometry for a simple two-pass heat exchanger.

The fluctuating jitter force can be approximated as an integral of the pressure fluctuation over the interior wall surface of a flow system:

$$F'(t)\approx\iint_{A_s} p'(x;t)\,\cos\theta(x)\,da\ . \tag{1}$$

The power spectral density of this fluctuating force follows as

$$\mathrm{PSD}_{F'}(\omega)\cong\iint_{A_s}\iint_{A_s}\phi^{1/2}(x_1;\omega)\phi^{1/2}(x_2;\omega)\rho(x_1;x_2;\omega)\times\cos\theta(x_1)\,\cos\theta(x_2)\,da_1\,da_2\ , \tag{2}$$

which is defined in terms of ϕ, the auto power spectral density of the fluctuating pressure, and ρ, the cross power spectral density correlation function. The correlation function is defined as

$$\rho(x_1;x_2;\omega)=\frac{\psi(x_1;x_2;\omega)}{[\phi(x_1;\omega)\phi(x_2;\omega)]^{1/2}}\ . \tag{3}$$

It is not uncommon for the range of $\rho(x_1;x_2;\omega)$ to be much smaller than the physical dimensions of the body whose jitter force is to be determined. In such cases it is useful to define a correlation area (assuming homogeneous turbulence):

$$A_{\eta,\zeta}(x)=\int_{-\infty}^{\infty}\int_{-\infty}^{\infty}\rho(x;\eta;\zeta;\omega)\,d\eta\,d\zeta\ , \tag{4a}$$

where η,ζ represent the longitudinal and transverse deviations from x. In most instances the available map of $\rho(x_1;x_2;\omega)$ will be incomplete. For such cases, a partial map is most likely to include pure longitudinal and pure transverse correlation lengths:

$$L_\eta(x)=\int_{-\infty}^{\infty}\rho(x;\eta,0,\omega)\,d\eta\ , \tag{4b}$$

$$L_\zeta(x)=\int_{-\infty}^{\infty}\rho(x;0,\zeta;\omega)\,d\zeta\ . \tag{4c}$$

The relationship among the definitions[12] implies that $A_{\eta,\zeta}\leq L_\eta L_\zeta$. Also, for the case of short-range correlation we have $\phi(x+\zeta;\omega)\approx\phi(x;\omega)$ and $\cos\theta(x+\zeta)\approx\cos x$. Then the PSD of the fluctuating force can be simplified:

$$\mathrm{PSD}_{F'}(\omega)\approx\iint_{A_s}\phi(x;\omega)L_\eta(x;\omega)L_\zeta(x;\omega)\,\cos^2\theta(x)\,da\ . \tag{5}$$

When applying Eq. (5) it is practical to assume that ϕ, L_η, and L_ζ are constant functions of position x, and furthermore that L_η and L_ζ are constant functions of frequency ω. Then the PSD of the jitter force can be approximated as

$$\mathrm{PSD}_{F'}(\omega)\approx L_\eta L_\zeta A_s\phi(\omega)\ , \tag{6}$$

where

$$A_s=\iint_{A_s}\cos^2\theta(x)\,da\ . \tag{7}$$

Data for ϕ are available in the literature in dimensionless form:

$$\Phi(\Omega)=\frac{2u}{dq^2}\phi(\omega)\ , \tag{8}$$

where Ω is the dimensionless frequency, $\Omega=\omega d/2u$, and $\Phi(\Omega)$ is the dimensionless pressure PSD. Examples of these dimensionless data sources are shown in Figs. 2 and 3(a).[12,13]

For many typical mirror manifold geometries, Φ will not be reported in the literature but the length variation of $(p'/q)^2$ will be available. Figure 4 shows an example for a sharp right-angle turn.[13] In the absence of resources to measure Φ, it is practical to assume a function Φ and scale it to the correct rms value by $(p'/q)^2_{\mathrm{rms}}$. These dimensionless func-

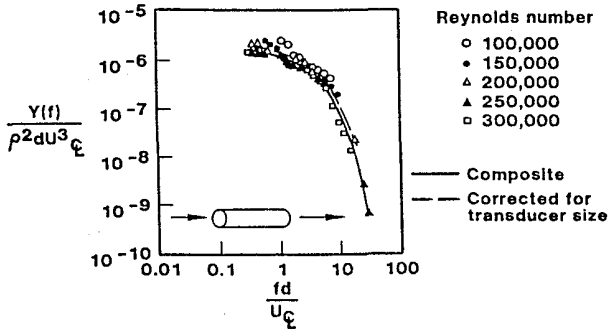

Fig. 2 Dimensionless pressure spectra for fully developed turbulent pipe flow.

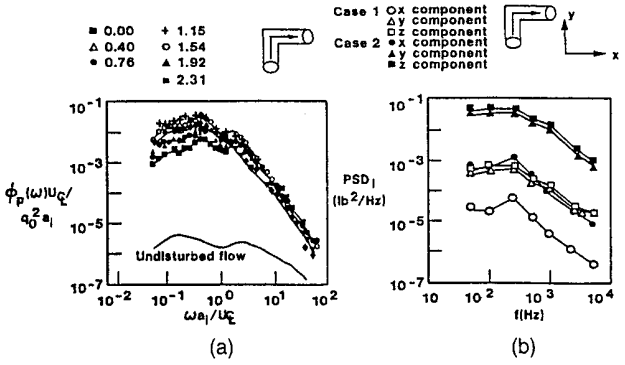

Fig. 3 (a) Dimensionless wall pressure spectra. (b) Tube force PSD.

tions can be substituted into Eq. (6) to reduce the jitter-force PSD to a form that is easily calculated from data that are currently available:

$$\mathrm{PSD}_{F'}(\omega) \approx L_\eta L_\zeta A_S \frac{q^2 d}{2u} \left(\frac{p'}{q}\right)^2_{\mathrm{rms}} \frac{\Phi(\omega)}{\Phi_0} \ . \tag{9}$$

The rms fluctuating force is computed by

$$(F')^2_{\mathrm{rms}} \approx \int \mathrm{PSD}_{F'}(\omega)\ \mathrm{d}\omega = L_\eta L_\zeta A_s q^2 \left(\frac{p'}{q}\right)^2_{\mathrm{rms}} \ , \tag{10}$$

and the fluctuating-force PSD can be written in terms of $(F')_{\mathrm{rms}}$:

$$\mathrm{PSD}_{F'}(\omega) \approx (F')^2_{\mathrm{rms}} \frac{d}{2u} \frac{\Phi(\Omega)}{\Phi_0} \ . \tag{11}$$

An example of the use of these equations is shown in Fig. 3(b), where the dimensionless data from the open literature,[12] shown in Fig. 3(a), have been substituted into Eq. (9). The result is a force PSD in engineering units for a pipe segment with a sharp right-angle turn. In Fig. 3(a), case 1 represents fully turbulent pipe flow, where the correlation area is $d^2/48$. Case 2 represents separated flow, where large eddies cause large correlation areas, from 20 to 100 times the value

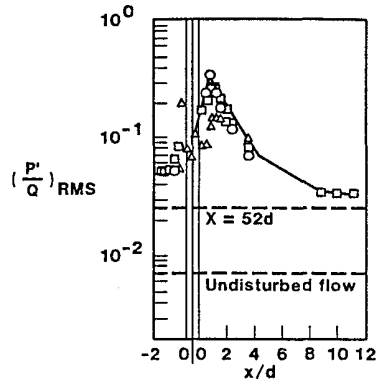

Fig. 4 Distribution of dimensionless rms pressure fluctuations with tube length for a sharp right-angle turn. Separation sources: sudden sharp turn, sudden expansion/contraction, orifice. High-pressure fluctuations persist 50 to 100 diameters.

in case 1. This example illustrates the potential for determining jitter forces for real hardware without measuring actual pressure fluctuations.

3 Flow-Induced Jitter Motion

The rigid-body motion of a mirror can be described by six independent degrees of freedom (DOFs), and the jitter motion of a mirror is adequately described by these rigid-body DOFs. The jitter motion is then related to the jitter force by a 6×6 transfer-function matrix $[H]$, where h_{ij} is the motion in the i direction due to the jitter force in the j direction. Each component is complex and a function of frequency. The jitter-motion PSD is completely defined by[66]

$$[\delta]_{\mathrm{PSD}} = [H][F]_{\mathrm{PSD}}[\mathrm{H}^*]^T \ , \tag{12}$$

where $[\delta]_{\mathrm{PSD}}$ and $[F']_{\mathrm{PSD}}$ are the jitter-motion and force matrices, respectively. Their diagonal elements represent auto power spectral densities, and the off-diagonal elements represent cross power spectral densities. The matrix $[H]$ can be computed by analytical methods for simple mirror-mount systems, computed by numerical methods such as finite-element analysis, or determined experimentally.

4 Vibration Control

The goal of jitter control is to reduce mirror motion and subsequent high-energy laser (HEL) beam error. This goal might be approached through active control techniques, for instance, by incorporating a fast-steering tilt mirror. However, the problem arises that the jitter-motion PSD may be distributed over a large bandwidth approaching 2000 Hz, and current tilt mirrors cannot control mirror motion to that high frequency. Further, sensor noise and control-system limitations make active beam control at very low jitter levels difficult even at much lower frequencies.

A more practical approach is to incorporate an understanding of the jitter-force phenomenon into the mirror design process to reduce jitter motion. Several techniques are available to the designer to improve the performance of the optic:

1. Adjust the parameters of the jitter-force equation (10) to reduce the force applied to the mirror.

2. Design a stiff mount to reduce the forced response of the mirror to the jitter force.
3. Use a stiff mount design together with a flexible no-load fitting to decouple the mirror from plumbing excitation caused by pumps, motors, ground vibrations, etc.
4. Add damping to the mirror-mount system to reduce the mirror response.

The parameters of the jitter force are defined by Eq. (10). These parameters are proportional to certain "controllable" flow variables such as the volume flow rate, coolant mass density, passage length, flow separation strength, number of passages, and total flow area. Substituting these variables into Eq. (10) gives

$$\text{Force PSD} \approx \frac{Q^3 \beta^2 L k}{NA} , \tag{13}$$

where

Q = coolant volume flow rate, m^3/s
β = coolant mass density, kg/m^3
L = conduit length, m
k = flow separation strength parameter
N = number of passages
A = total flow area, m^2 .

Thus the jitter force can be reduced as shown in Eq. (13) by using a lower-density coolant (ammonia rather than water), using shorter conduits, using large inlet flow areas with as many inlet tubes as possible, and (especially) designing for a lower flow rate. Also, eliminating flow-separation geometries within the mirror, where possible, reduces the overall force acting on the mirror. For instance, tapered expansions could be used instead of orifices, and corners could be rounded instead of sharp.

When the mirror is constrained in a mount system, the mirror response is described by the narrowband response[67]

$$Z_{\text{rms}}^2 = \frac{1}{64\zeta\pi^3} \frac{F_{\text{PSD}}(f_n)}{m^2 f_n^3} . \tag{14}$$

Given that observations show that the force PSD is usually a constant or decreasing function of frequency, then raising the natural frequency of the mirror-mount system, f_n, will reduce the magnitude of the mirror response Z. More specifically, increasing the stiffness of the mount, for a given mass m, will decrease the mirror response.The key to low-jitter mount design is to design for a first mount resonance that is as high as possible. While it is possible to match a higher-frequency disturbance with a high mirror resonance, such disturbances are usually smaller in magnitude, and turbulence excitation is usually sufficiently broadband to excite any lower mirror resonances much more than higher ones. In practice, first resonance has been found to be an effective and reachable goal.

Making the mount stiffer has another advantage: it isolates mechanical-borne vibration of the plumbing from the mirror. Mechanical-borne vibration can arise from a variety of sources, including pumps, motors, blowdown facilities, water chillers, and acoustic noise. The mount stiffness attenuates the plumbing motion by reacting out the excitation load through the base. In many cases, the mirror is mounted separately from the coolant supply lines, which are supported by a coolant coupling support bracket. The support bracket reacts the plumbing excitation loads without providing a direct load path to the mirror. These designs also incorporate a pressure-balanced coolant transfer fitting, or "no-load" fitting, that eliminates axial static pressure forces and attenuates dynamic jitter forces from the mirror and the mount that supports the mirror through the flexible O ring. The no-load fitting shown in Fig. 5 uses a pressure-force reacting piston that is mounted to the support bracket. This piston transfers the axial static pressure and dynamic jitter loads to the bracket, thus isolating the mirror and its mount from these loads. The no-load fitting is mounted in the support bracket in a self-adjusting ball joint that prevents mechanical-borne loads from being transmitted to the mirror. Summarizing, the mirror can be isolated from both mechanical- and fluid-borne plumbing excitations by providing an excitation load path away from the mirror.

Another technique can be applied in the design of the mount to reduce mirror jitter motion: constrained-layer damping of the mount. This technique has been developed and applied to pulsed-laser resonator optics to damp out mirror motion caused by a periodic pressure pulse.[68] Similarly, constrained-layer damping could be used to minimize the mirror response to internally generated jitter forces. As stated earlier, the response of the mirror-mount system is narrowband, and the maximum resonant response of the mirror is inversely proportional to the mount damping ratio ζ. This ratio in turn is proportional to the strain energy dissipated by the viscoelastic material in a vibration mode.[69] The design of the mount can effectively utilize damping to maximize ζ. In one design of a pulsed chemical laser mirror, a mirror-mount system achieved damping ratios on the order of 15%, two orders of magnitude greater than that of an undamped mount.

5 Jitter Forces in Coolant Flow Systems

A pioneering study of coolant-flow-induced forces in a large system was carried out at the AFWL on the Airborne Laser Laboratory (ALL).[70,71] The primary techniques used to reduce a large-system jitter problem included the use of showerhead orifices, flexible hoses, and mechanical isolation of certain parts of the system. A 75% reduction of system jitter was subsequently accomplished. A study to characterize the

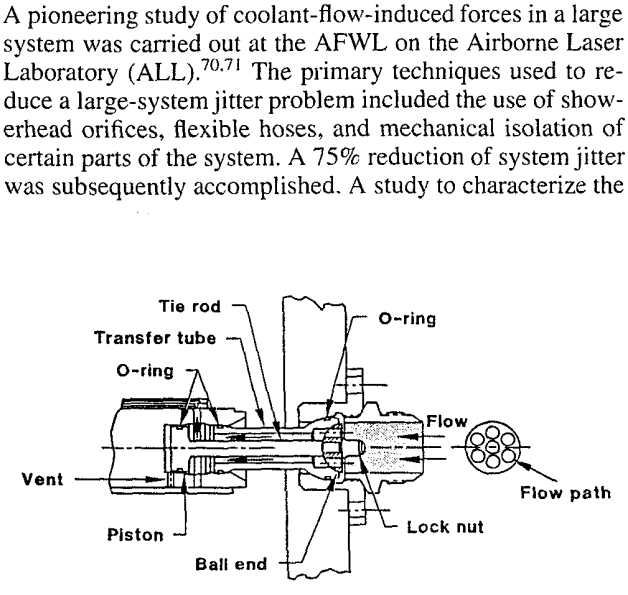

Fig. 5 Load-balanced coolant fitting used for plumbing isolation.

ALL jitter and predict its magnitude from known disturbances and system dynamic characteristics was later carried out.[72]

The key factor in determining the presence and magnitude of coolant-flow-induced forces is the flow Reynolds number $\mathrm{Re}=ur/v$, where v is the kinematic viscosity, u the mean flow velocity, and r the pipe radius. For $\mathrm{Re}<2000$, laminar flow will exist and forces are greatly reduced. For $\mathrm{Re}>4000$, the flow will be turbulent, and significant-flow induced forces are possible. Flow perturbations such as sudden diameter changes, valves, and orifices cause flow separation and large flow-induced forces. Nominally laminar flow will allow rapid reattachment of flow, minimizing the perturbation effects, whereas turbulent flow will prevent flow reattachment and will propagate the forces for hundreds of pipe diameters downstream of the perturbations. Determination of the magnitude and spectrum of these flow-induced forces is possible by employing the method outlined above and dimensionless published data. References that are particularly useful in calculating the jitter forces caused by flow perturbations such as sudden diameter changes and right-angle turns include Bull and Norton[13] and Mabey.[51] To counter the effects of pressure fluctuations produced by pumps, Carey[58] describes the successful design and construction of an acoustic filter in detail. Although the standard practice has been to use a pressurized blowdown coolant system to avoid pump pressure fluctuations, Carey's work shows that pumps can be used successfully.

6 Measurement of Jitter Forces

The jitter force is related to the jitter motion by

$$[A]=[H][F][H^*]^T \ , \tag{15}$$

where $[A]$ is the acceleration matrix and is measured directly as discussed above. This equation assumes that $[H]$ is not a function of flow, which may not be true in all cases. The diagonal elements of $[A]$ represent the auto power spectral densities, and the off-diagonal terms of $[A]$ represent the cross power spectral densities. The transfer-function matrix $[H]$ is also measured directly using the impact hammer technique. The components h_{ij} represent the output acceleration of DOF i divided by the impact force in DOF j; h_{ij} is defined in the frequency domain. The output acceleration is measured with special low-noise accelerometers, and the impact force is measured using a quartz force transducer on the impact hammer. The components h_{ij} are computed using a spectrum analyzer. The jitter forces are calculated by computing the inverse of the transfer-function matrix and its complex conjugate, and pre- and postmultiplying Eq. (15) by $[H]^{-1}$ and $[H^*]^{-T}$, respectively. The resulting equation for the jitter force matrix is

$$[F]=[H]^{-1}[A][H^*]^{-T} \ . \tag{16}$$

The diagonal elements of $[F]$ represent the force auto power spectral densities, and the off-diagonal terms represent the cross power spectral densities. The matrix $[H]$ contains all the structural dynamic information of the mirror-mount system as flow tested, and therefore accounts for all system resonances. Figure 6 shows an example of how the matrix [TF] (or $[H]$) accounts for a system resonance at 200 Hz, and removes the peak in the response data from the force

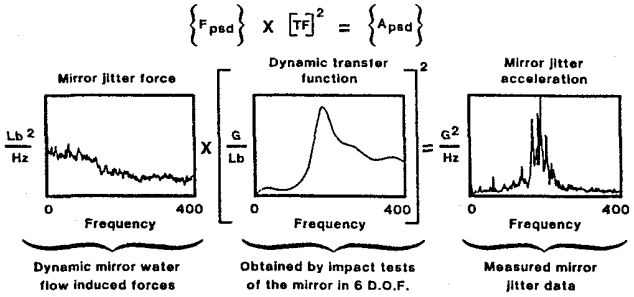

Fig. 6 Data-reduction technique that removes mirror-mount resonant response from jitter-force PSDs.

PSD. Without using such a technique, force PSDs are inevitably colored by mount-system resonances.

During the period from 1983 to 1990, a number of flow tests were carried out on a wide variety of optics in which the procedures described above were utilized.[73–80] The mirrors evaluated included conventional channel flow, hole scraper, heat pipe, phase-change, and low-velocity cooled glass types. The published data are similar to the curves shown in Fig. 8 and can be useful in designing suitable mirror mounts.

7 Design Example: a Typical Two-Pass Mirror

The mirror selected for analysis is one with a typical two-pass heat exchanger and represents a good example of how the various aspects of jitter control analysis are integrated together in the actual design, analysis, and testing of a mirror. The mirror is 13 in. in diameter with the following coolant flow characteristics: 50-gal/min flow rate, 450-psi inlet pressure, 50-psi exit pressure. The mirror had a design goal that the RSS total of the rms jitter rotations around three axes was to be less than 0.72 μrad. The design procedure was:

1. Determine the jitter force acting on the mirror.
2. Design the mirror-mount system for low response.
3. Determine the response of the system and whether the design goal is satisfied.
4. Verify the analytical predictions of jitter force and motion by testing the mirror system hardware.

A cutaway view of the mirror is shown in Fig. 7, identifying the locations of flow separation by shading. The jitter force is computed by assuming that these are independent, uncorrelated turbulence sources. The force PSD of each independent source is determined using Eq. (9), and these PSDs are RSS'd in a global coordinate frame.[1] The resulting force PSD is listed in Table 1.[81] The forces acting on the mirror and on the coolant supply fitting are tabulated separately. A graphical summary of the force rms for various locations is also shown in Fig. 7, and it is evident that manifolding is the dominant source of jitter forces.

The force contribution from the heat exchanger of the mirror is negligible compared to the contribution of the coolant inlet and exit ports and manifolding. This is because the flow through a single manifold is the same as that through the entire heat exchanger, but the number of conduits [N in Eq. (13)] is 400 times larger. So the total heat-exchanger

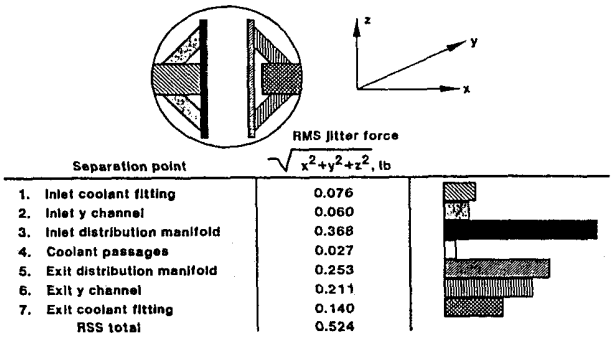

Fig. 7 Distribution of jitter forces within a typical high-energy laser mirror.

Table 1 Coolant-flow-induced loads.

	MIRROR			COOLANT SUPPLY FITTING		
FREQ	PSD_X	PSD_Y	PSD_Z	PSD_X	PSD_Y	PSD_Z
Hz	lb^2/Hz	lb^2/Hz	lb^2/Hz	lb^2/Hz	lb^2/Hz	lb^2/Hz
5	9.25 E-5	8.18 E-5	1.07 E-5	0	1.23 E-6	1.23 E-6
10	1.68 E-4	7.13 E-5	7.15 E-5	0	2.87 E-6	2.87 E-6
100	1.75 E-4	7.14 E-5	6.25 E-4	0	2.99 E-6	2.99 E-6
200	1.94 E-4	6.21 E-5	2.13 E-5	0	1.23 E-6	1.23 E-6
400	1.37 E-4	3.30 E-5	4.16 E-5	0	3.59 E-7	3.59 E-7

force contribution for 400 passages is only 7% of the force contribution from one manifold slot, and the heat-exchanger contribution becomes a small percentage of the total mirror force. This implies that the mirror designer should focus his concern on reducing flow separation points in the inlet and exit ports and mirror manifolding.

A comparison between theoretically calculated and measured jitter forces is shown in Fig. 8. It is evident that although the fine structure of the PSDs cannot be predicted without more detailed calculations, the magnitude and frequency trends of the predictions are remarkably close to the test data.

The mirror mount was designed using the second technique discussed herein: provide a high mirror-mount system resonance to reduce jitter response. A design goal was established that the fundamental mirror-mount system resonance was to be above 200 Hz. Previous experience has proven that such a system provides a stable response with low jitter motion, and is an achievable goal. The conceptual design of the mount, shown in Fig. 9, consisted of a 3-in. base plate supported on four legs. The mirror supports and water-hose supports are attached to a 1.5-in. top plate, which rests on a 1.5-in. intermediate plate. A NASTRAN finite-element model was used to complete a modal analysis of the conceptual design. Several design iterations were made until the first resonance was raised to 170 Hz, a good first approximation of the 200-Hz goal. A NASTRAN forced-response analysis was then used to determine the mirror-mount system response to the input loads listed in Table 1. The rms responses (0–500 Hz) calculated by NASTRAN for the mirror are summarized in Fig. 10. The total RSS system response was estimated to be 0.067 μrad, well below the 0.720-μrad goal.

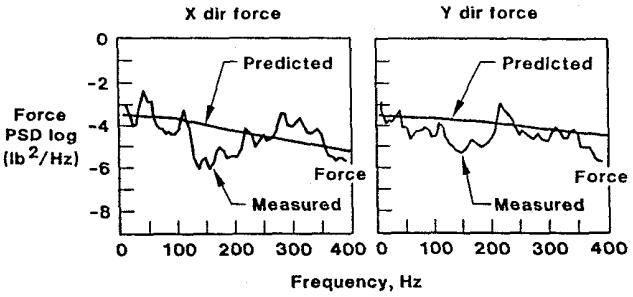

Fig. 8 Predicted jitter force PSDs are close to measured values from flow tests.

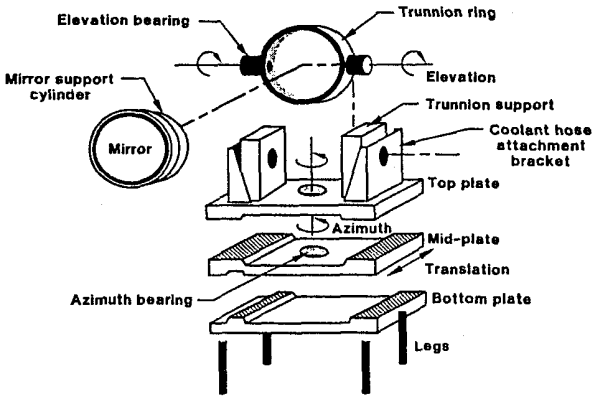

Fig. 9 A low-jitter mount design with plumbing isolation and high stiffness.

The mirror and mount were instrumented, and the coolant-flow-induced mirror motion and forces were measured. The accelerations are related to the impact forces by the measured transfer function matrix $[H]$:

$$\{A\}=[H]\{F\} \ . \tag{17}$$

The impact forces are related to the six independent global forces by the matrix $[G]$:

$$\{F_G\}=[G]\{F\} \ . \tag{18}$$

Now, the acceleration can be expressed as a function of the global forces by inverting Eq. (18) and substituting in Eq. (17):

$$\{A\}=[H][G]^{-1}\{F_G\} \ , \tag{19}$$

$$\{A\}=[D]\{F_G\} \ . \tag{20}$$

Finally, the force PSD can be expressed in terms of the measured acceleration PSD and modified transfer function matrix by

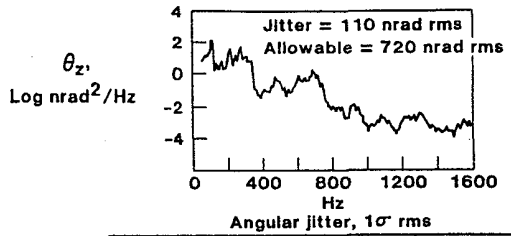

Angular jitter, 1σ rms

	θ_x, nrad	θ_y, nrad	θ_z, nrad	Total, nrad
Predicted	51	27	34	67
Measured	51	59	73	110
Allowable				720

Fig. 10 Mirror jitter PSD from flow test; comparison of predicted, measured, and allowable rms jitter.

$$\{F_G\}_{PSD} = [D]^{-1}\{A\}_{PSD}[D^*]^{-T} \quad . \tag{21}$$

The measured motion and forces agreed well with the analytical predictions, and the measured displacements were well below the 0.720-μrad design goal. These results are summarized and plotted in Fig. 10.[82] The RSS angular displacement is 0.110 μrad, well below the 0.720-μrad goal. Although the predicted jitter of 0.067 μrad was significantly lower than the 0.110-μrad value, it correctly predicted that the performance would meet the design goal by a wide margin. Thus the utility of this design approach has been clearly shown, and a similar procedure is recommended for use by the community.

8 Conclusions

The preceding sections have developed a theoretical basis for calculating coolant-flow-induced jitter forces, illustrated how to calculate forces from previously published data, showed how to measure jitter forces and compared data with predictions, listed the major factors controlling jitter forces, and demonstrated the importance of high-stiffness mount design in achieving design jitter goals. The following conclusions can be drawn from these developments:

1. Coolant-flow-induced forces can be minimized by:
   a. controlling flow parameters
   b. avoiding separation from orifices, valves, and turns
   c. minimizing flow dynamic head
   d. careful mirror design
   e. calculating jitter forces.
2. Low jitter mounts are achieved by:
   a. isolating plumbing
   b. designing for 200-Hz first resonance
   c. calculating jitter forced response and redesigning if necessary.
3. Jitter forces can be calculated on an absolute basis without adjustment factors.
4. Jitter forces can be measured independently of mount resonances.

9 Nomenclature

a_i = radius of pipe i
A = total flow area
$A_{\eta,\zeta}$ = correlation area over longitudinal and transverse x deviations
d = pipe diameter
da_i = differential area i
$[F']_{PSD}$ = matrix of force PSDs
$F'(t)$ = fluctuating jitter force due to wall pressure fluctuations
$[G]$ = matrix relating impact forces to global forces
$[H]$ = frequency-dependent dynamic transfer-function matrix
k = flow separation parameter
L = conduit length
L_ζ = transverse correlation length
L_η = longitudinal correlation length
N = number of passages
$p'(x;t)$ = wall pressure fluctuations with time at position x
PSD(ω) = power spectral density of fluctuating force
q = dynamic pressure, $1/2\ \rho u^2$
Q = coolant volume flow rate
Re = Reynolds number
u = pipe mean flow velocity
U_c = centerline flow velocity
x_i = distance in the i direction
$y(f)$ = see $\phi(x,w)$ below

Greek

β = coolant mass density
$[\delta]_{PSD}$ = matrix of motion PSDs
ζ = critical damping ratio
θ = circumferential angle inside a tube
$\rho(x_1;x_2;\omega)$ = cross power density correlation function
$\phi(x,\omega)$ = auto power spectral density of pressure at position x
$\Phi(\Omega)$ = dimensionless auto power spectral density of pressure
$\psi(x_1;x_2;\omega)$ = local cross power spectral density of pressure
ω = circular frequency
Ω = dimensionless frequency, $wd/2u$

Acknowledgments

The basic research into flow-induced jitter phenomena was sponsored by the United Technologies Research Center, the United Technologies Optical Systems Division, and DARPA. The author is especially indebted to Dr. R. K. Irey, Mr. R. G. Jaeger, and Mr. E. Moas, Jr.

References

1. R. K. Irey, "Flow induced jitter forces," *Report 82R-182503-01*, United Technologies Research Center* (Aug. 1982).
2. F. M. White, *Vicous Fluid Flow*, McGraw-Hill, New York (1974).
3. H. Schlichting, *Boundary Layer Theory*, 6th ed., McGraw-Hill, New York (1966).
4. J. O. Hinze, *Turbulence*, McGraw-Hill, New York (1959).
5. Private Communication; unpublished report entitled "HQM jitter analysis."*
6. G. M. Corcos, "The structure of the turbulent pressure field in boundary layer flows," *J. Fluid Mech.* **18**(3), 353–378 (1964).

*Government or company report with limited distribution. Interested readers should contact the appropriate institution for more information.

7. W. W. Willmarth, "Pressure fluctuations beneath turbulent boundary layers," in *Ann. Rev. of Fluid Mechanics*, Van Dyke, W. G. Vincenti, and J. V. Wehausen, Eds., Vol. 7, pp. 13–37, Annual Reviews Inc., Palo Alto, CA (1975).
8. R. H. Kraichnan, "Pressure fluctuations in turbulent flow over a flat plate," *J. Acoust. Soc. Am.* **28**(3), 378–390 (1956).
9. R. H. Kraichnan, "Pressure field within homogeneous anisotropic turbulence," *J. Acoust. Soc. Am.* **28**(1), 64–72 (1956).
10. W. C. Meecham, and M. T. Travis, "Theoretical pressure correlation functions in turbulent boundary layers," *Phys. Fluids* **23**(6), 1119–1131 (1980).
11. R. L. Panton and J. H. Linebarger, "Wall pressure spectra calculations for equilibrium boundary layers," *J. Fluid Mech.* **65**(2), 261–287 (1974).
12. H. P. Bakewell, G. F. Carey, J. J. Libaha, H. H. Schloemer, and W. A. Von Winkle, "Wall pressure correlation in turbulent pipe flow," Report 559, USL, (Aug. 1962).
13. M. K. Bull and M. D. Norton, "On the hydrodynamic and acoustic wall pressure fluctuations in turbulent pipe flow due to a 90° mitred bend," *J. Sound Vibr.* **76**(4), 561–586 (1981).
14. F. R. Fricke, and D. C. Stevenson, "Pressure fluctuations in a separated flow region," *J. Acoust. Soc. Am.* **44**(5), 1189–1200 (1968).
15. H. H. Bruun and B.O.A.L. Davies, "An experimental investigation of the unsteady pressure forces on a circular cylinder in a turbulent cross flow," *J. Sound Vibr.* **40**(4), 535–559 (1975).
16. J. Laufer, "The structure of turbulence in fully developed pipe flow," Report 1174, National Advisory Committee for Aeronautics 1954.
17. R. E. Britter, J. C. R. Hunt, and J. C. Mumford, "The distortion of turbulence by a circular cylinder," *J. Fluid Mech.* **92**(2), 269–301 (1979).
18. J. S. Bendat and A. G. Piersol, *Measurement and Analysis of Random Data*, Wiley, New York (1966).
19. E. J. Richards and D. J. Mead, *Noise and Acoustic Fatigue in Aeronautics*, Wiley, New York (1968).
20. P. Bradshaw, *An Introduction to Turbulence and Its Measurement*, Pergamon (1971).
21. W. W. Willmarth, and C. E. Wooldridge, "Measurements of the fluctuating pressure at the wall beneath a thick turbulent boundary layer," *J. Fluid Mech.* **14**(2), 187–210 (1962).
22. H. P. Bakewell, "Turbulent wall-pressure fluctuations on a body of revolution," *J. Acoust. Soc. Am.* **43**(6), 1358–1363 (1968).
23. M. K. Bull, "On the form of the wall-pressure spectrum in a turbulent boundary layer in relation to noise generation by boundary layer–surface interactions," in *Joint Symp. on Mechanics of Sound Generation in Flows*, E. A. Muler, Ed. Springer-Verlag, Göttingen pp. 210–216 (Aug. 1979).
24. J. P. Batham, "Pressure distributions on circular cylinders at critical Reynolds numbers," *J. Fluid Mech.* **57**(2), 209–228 (1973).
25. F. A. Aupperle and R. F. Lambert, "Effects of roughness on measured wall pressure fluctuations beneath a turbulent boundary layer," *J. Acoust. Soc. Am.* **47**(2), 359–370 (1970).
26. P. J. Mulhearn, "Turbulent boundary layer wall-pressure fluctuations down-stream of an abrupt change in surface roughness," *Phys. Fluids* **19**(6), 796–801 (1976).
27. E. J. Skudrzyk, "Noise production in a turbulent boundary layer by smooth and rough surfaces," *J. Acoust. Soc. Am.* **32**(1), 19–33 (1960).
28. G. M. Corcos, "Resolution of pressure in turbulence," *J. Acoust. Soc. Am.* **35**(2), 192–199 (1963).
29. F. E. Geib, "Measurements on the effects of transducer size on the resolution of boundary-layer pressure fluctuations," *J. Acoust. Soc. Am.* **46**(2), 253–261 (1969).
30. R. B. Gilchrist, "Experimental hydrophone-size correction factor for boundary-layer pressure fluctuations," *J. Acoust. Soc. Am.* **38**, 298–302 (1965).
31. W. W. Willmarth, "Space-time correlations of the fluctuating wall pressure in a turbulent boundary layer," *J. Aero. Sci.*, pp. 335–336 (May 1958).
32. W. W. Willmarth, "Wall pressure fluctuation in a turbulent boundary layer," *J. Acoust. Soc. Am.* **28**(6), 1048–1053 (1956).
33. W. W. Willmarth and C. S. Yang, "Wall-pressure fluctuations beneath turbulent boundary layers on a flat plate and cylinder," *J. Fluid Mech.*, **41**(1), 47–80 (1970).
34. W. W. Willmarth, and F. W. Roos, "Resolution and structure of the wall pressure field beneath a turbulent boundary layer," *J. Fluid Mech.* **22**(1), 81–84 (1965).
35. J. A. Elliott, "Microscale pressure fluctuations measured within the lower atmospheric boundary layer," *J. Fluid Mech.* **53**(2), 351–383 (1972).
36. R. Emmerling, G.E.A. Meier, and A. Dimkelacker, "Investigation of the instantaneous structure of the wall pressure under a turbulent boundary layer flow," in *Conf. on Noise Mechanisms*, pp. 24-1–24-12, AGARD C.P. 131, Brussels, Sept. 1973.
37. M. K. Bull and A.S.W. Thomas, "High frequency wall-pressure fluctuations in turbulent boundary layers," *Phys. Fluids* **19**(4), 597–599 (1976).
38. M. K. Bull, "Wall-pressure fluctuations associated with subsonic turbulent boundary layer flow," *J. Fluid Mech.* **28**(4), 719–754 (1967).
39. J.A.B. Wills, "Measurements of the wave-number/phase velocity spectrum of wall pressure beneath a turbulent boundary layer," *J. Fluid Mech.* **45**(1), 65–90 (1970).
40. H. H. Schloemer, "Effects of pressure gradients on turbulent-boundary layer wall-pressure fluctuations," *J. Acoust. Soc. Am.* **42**(1), 93–113 (1966).
41. P. Bradshaw, "Interactive motion and pressure fluctuations in turbulent boundary layers," *J. Fluid Mech.* **30**(2), 241–258 (1967).
42. L. Goodman and A. Massey, "Pressure induced by a stagnating turbulent field," *Phys. Fluids* **19**(7), 1061–1062 (1976).
43. H. V. Fuchs, "Measurement of pressure fluctuations within subsonic turbulent jets," *J. Sound Vibr.* **22**(3), 361–378 (1972).
44. H. V. Fuchs, "Resolution of turbulent jet pressure into azmuthal components," in *Conf. on Noise Measurements*, pp. 27-1–27-10, AGARD C.P. 131, Brussels (1973).
45. P. W. Bearman, "On vortex shedding from a circular cylinder in the critical Reynolds number regime," *J. Fluid Mech.* **37**(3), 577–585 (1969).
46. Y. C. Fung, "Fluctuating lift and drag acting on a cylinder in a flow at supercritical Reynolds numbers," *J. Aerospace Sci.* **27**(11), 801–814 (1960).
47. P. W. Bearman, "On vortex street wakes," *J. Fluid Mech.* **28**(4), 625–641 (1967).
48. P. A. Durbin and J.C.R. Hunt, "On surface pressure fluctuations beneath turbulent flow round bluff bodies," *J. Fluid Mech.* **100**(1), 161–184 (1980).
49. F. R. Fricke, "Pressure fluctuations in separated flows," *J. Sound Vib.* **17**, (1) 113–123 (1971).
50. E. M. Greshilov, A. V. Evtushemko, and L. M. Lyamshev, "Spectral characteristics of the wall pressure fluctuations associated with boundary layer separation behind a projection on a smooth wall," *Sov. Phys. Acoust.* **15**(1), 29–34 (1969).
51. D. G. Mabey, "Analysis and correction of data on pressure fluctuations in separated flow," *J. Aircraft* **9**(9), 642–645 (1972).
52. A. M. Mohsen, "Experimental investigation of the wall pressure fluctuations in subsonic separated flows," Report D6-17094 AD 669214, Boeing Co. Commerical Airplane Div. (Jan. 1967).
53. H. Rouse and V. Jezdinsky, "Fluctuation of pressure in conduit expansions," Paper 4815, *Proc. ASCE J. Hydraulics Div.* **92**(Hy 3), 1–12 (1966).
54. M. K. Bull and M. D. Norton, "The proximity of coincidence and acoustic cut-off frequencies in relation to acoustic radiation from pipes with disturbed internal turbulent flow," *J. Sound Vib.* **69**(1), 1–11 (1980).
55. M. J. Tunstall, and J. K. Harvey, "On the effect of a sharp bend in a fully developed turbulent pipe-flow," *J. Fluid Mech.* **34**(3), 595–608 (1968).
56. Airborne Laser Laboratory Cycle III and IV Support Services, "Water flow induced jitter investigation," Report FR 11388, Pratt and Whitney Aircraft Group, Government Products Div. (June 1979).
57. P. W. Bearman, "Some measurements of the distortion of turbulence approaching a two-dimensional bluff body," *J. Fluid Mech.* **53**(3), 451–467 (1972).
58. G. F. Carey, "Acoustic turbulent water flow tunnel," *J. Acoust. Soc. Am.* **41**(2), 373–379 (1967).
59. R. M. Hoover, D. T. Laird, and L. N. Miller, "Acoustic filter for water-filled pipes," *J. Acoust. Soc. Am.* **22**(1), 38–41 (1958).
60. W. W. Willmarth, "Unsteady force and pressure measurements," *Ann. Rev. Fluid Mech.* **3**, 147–170 (1971).
61. W. K. Blake, "Turbulent boundary-layer wall pressure fluctuations on smooth and rough walls," *J. Fluid Mech.* **44**, 637–660 (1970).
62. P.F.R. Weyers, "Vibration and near-field sound of thin-walled cylinders caused by internal turbulence flow," *Report TN-D-430, NASA* (June 1960).
63. J. M. Chenoweth and J. R. Stenner, "Flow-induced heat exchanger tube vibration—1980," HTD Vol. 9, Amer. Soc. Mech. Engrs. (Nov. 1980).
64. J. Scheiman, "Comparison of experimental and theoretical turbulence reduction characteristics for screens, honeycomb, and honeycomb screen combinations," Technical Paper 1958, NASA (1981).
65. R. D. Blevins, *Flow Induced Vibration*, Van Nostrand, 1977.
66. Y. K. Lin, *Probabilistic Theory of Structural Dynamics*, Chapter 6, R. E. Krieger, Malabar, FL (1976).
67. C. M. Harris, and C. E. Crede, *Shock and Vibration Handbook*, 2nd ed., Chapter 11, McGraw-Hill, New York (1976).
68. R. G. Jaeger, "Dynamic response of Boeing uncooled repetitively pulsed laser mirrors," Report 82-5322-035, United Technologies Research Center, Optics and Applied Technology Laboratory, (June 1983).*
69. C. D. Johnson, D. A. Klenholz, and L. C. Roger, "Finite Element Prediction of Damping in Beams with Constrained Layer Damping."*

*Government or company report with limited distribution. Interested readers should contact the appropriate institution for more information.

70. P. D. McQuade, "An investigation of flow-induced vibrations of the water-cooled laser mirrors of the U.S. Air Force Airborne Laser Laboratory," TN 79-002 AFWL/LR, (Apr. 1979).
71. C. A. Sudduth, "Water flow induced jitter investigation," Report FR-11388, Airborne Laser Laboratory Cycle III and IV Support Services, Pratt and Whitney (June 1979).*
72. J. Jeter, et al. "Jitter prediction," Report TR-84-136 AFWL (June 1985).
73. R. G. Jaeger, "TRW it's Hale scraper mirror water flow jitter tests data analysis and results," Report 83-5599-035, United Technologies Research Center (Apr. 1983).*
74. "ALPHA inner axicon jitter test," Critical Design Review, TRW (Apr. 1983).*
75. R. G. Jaeger, "Lode secondary mirror Jitter Test Program Final Report," Report 83R-981181-01, United Technologies Research Center (Dec. 1983).*
76. E. Moas, Jr., "Laser mirror flow induced vibration forces," Report 85R-981262-01, United Technologies Research Center (Feb. 1985).*
77. C. B. Jones, "Heat pipe jitter test final report," Report 85R-981485-01, United Technologies Research Center (Oct. 1985)*
78. K. Fletcher, "Cooled glass mirror flow induced jitter tests," Report 87-6076-03S, United Technologies Optical Systems (Sept. 1987).*
79. K. Fletcher, "Phase change cooled mirror jitter test report," Report 90R-982903-01, United Technologies Optical Systems (Jan. 1990).*
80. E. Moas, Jr., "Coolant flow induced jitter analysis," Report 83-5328-01S, United Technologies Research Center (May 1984).*
81. K. T. Fletcher, "Dynamic response analysis of 13 inch SM mirror for coolant flow induced loads," Report 83-5288-015 United Technologies Research Center, Optics and Applied Technology Laboratory, (Apr. 1983).*
82. K. T. Fletcher, "Measurement of the coolant flow induced jitter forces and displacements of the 13 inch SM mirror," Report 85-5288-053 United Technologies Research Center, Optics and Applied Technology Laboratory (July 1985).*

Michael J. Laughlin has worked in the high-energy laser/optical structures field with United Technologies Corporation from 1973 to 1994. During the 1970s, he worked extensively on the successful A.L.L. jitter force reduction program at the Air Force Weapons Laboratory in New Mexico. During the early 1980s, he sponsored Dr. R.K. Irey's pioneering work in flow-induced jitter force prediction, developed computer programs to apply theory to real mirror configurations, and developed several low-jitter mirror designs. In addition he developed the jitter force measurement technology and directed a series of pioneering jitter force measurement tests at United Technologies Research Center/Optics and Applied Technology Laboratory. The jitter force prediction theory and the corroborating jitter force measurement tests have been successfully applied to several low-jitter optics and coolant supply systems.

*Government or company report with limited distribution. Interested readers should contact the appropriate institution for more information.